

Possibility of BCS-BEC crossover in κ -type organic superconductors

Hiroshi Watanabe^{1,2,*} and Hiroaki Ikeda³

¹*Department of Liberal Arts and Basic Sciences,*

College of Industrial Technology, Nihon University, Chiba 275-8576, Japan

²*Research Organization of Science and Technology, Ritsumeikan University, Shiga 525-8577, Japan*

³*Department of Physical Science, Ritsumeikan University, Shiga 525-8577, Japan*

(Dated: November 26, 2024)

The realization of BCS-BEC crossover in superconductors, which smoothly connects Bardeen-Cooper-Schrieffer (BCS) theory with Bose-Einstein Condensation (BEC) in fermion systems, is an intriguing recent topic in strongly correlated electron systems. The organic superconductor κ -(BEDT-TTF)₄Hg_{2.89}Br₈ (κ -HgBr) under pressure is one of the leading candidates, owing to its unique metallic spin-liquid nature and tunable electron correlation. We theoretically investigate the extended Hubbard model for κ -HgBr and discuss the possibility of the BCS-BEC crossover by systematically calculating superconducting correlation function, coherence length, superfluid weight, and chemical potential. Our findings show that the BCS-BEC crossover can be observed when competing phases, such as Mott insulators and charge and/or spin orders, are suppressed by appropriate hole doping. κ -HgBr is just the case because both the Mott insulating phase and magnetic orders are absent due to its nonstoichiometric Hg composition and geometrical frustration. We further propose that other κ -type organic superconductors could serve as potential candidates of the BCS-BEC crossover if their band fillings are systematically tuned.

Introduction— Superconductivity (SC), even over a century after its discovery, continues to present compelling research opportunities in condensed matter physics. Possibility of a crossover from BCS (Bardeen-Cooper-Schrieffer) type to BEC (Bose-Einstein Condensate) type behavior [1] in solid-state materials is one of the recent intriguing topics. Although the BCS-BEC crossover has been established in ultracold atom systems [2–5], most SC in solid-state materials is considered to reside in the BCS regime; criteria for BCS-BEC crossover, such as $\Delta/E_F \sim 1$ (superconducting gap Δ comparable to the Fermi energy E_F) or $k_F\xi \sim 1$ (coherence length ξ comparable to the average interparticle distance $\sim 1/k_F$), are typically not met. Recently, however, various strongly correlated materials, including iron-based superconductors [6, 7], organic superconductors [8], two-dimensional gated semiconductors [9], and even cuprate superconductors [10], have been proposed to lie in the BCS-BEC crossover region. In addition to meeting the criteria mentioned above, these materials exhibit pseudogap behavior [9] or flattened band dispersions [7], both of which are characteristic features of the BCS-BEC crossover.

In strongly correlated electron systems, realizing BCS-BEC crossover poses several challenges: i) The range over which interactions can be controlled by physical or chemical pressure is limited compared with the Feshbach resonance used for ultracold atoms. ii) Competing phases, such as Mott insulators and charge and/or spin orders, are often present. These competing phases generally mask SC, preventing its realization. iii) Multi-orbital effects, which frequently produce nontrivial phenomena in strongly correlated electron systems, add further complexity, making the identification of the BCS-BEC crossover challenging [7, 11].

Despite these challenges, the quasi two-dimensional organic superconductor κ -(BEDT-TTF)₄Hg_{2.89}Br₈ (κ -HgBr) [12, 13] under pressure has emerged as a promising candidate for realizing BCS-BEC crossover. Owing to the tunability of its lattice constant and bandwidth by pressure, electron correlation in κ -HgBr can be controlled more easily than in inorganic materials. The superconducting transition temperature T_c shows a dome-shaped pressure dependence, and non-Fermi-liquid behavior is observed on the low-pressure (strongly correlated) side [14, 15], both of which indicate the potential for BCS-BEC crossover near the T_c peak. The estimated in-plane coherence length $k_F\xi_{\parallel}$ ranges from approximately 3 (BEC-like at 0.24 GPa) to 50 (BCS-like at 1.0 GPa) [8], further suggesting a pressure-induced BCS-BEC crossover. κ -HgBr is also notable as a candidate for a doped quantum spin liquid (QSL) [15], exhibiting metallic properties due to its nonstoichiometric Hg composition of 2.89. The absence of neighboring magnetic orders and Mott insulators is favorable for realizing BCS-BEC crossover. Additionally, the band structure around the Fermi energy is relatively simple and free from complex multi-orbital effects, enhancing its suitability for this crossover.

As discussed above, κ -HgBr is considered an ideal system for realizing BCS-BEC crossover. In this paper, we theoretically investigate the possibility of BCS-BEC crossover in κ -HgBr and related organic superconductors. We introduce a four-band extended Hubbard model as an effective low-energy model, and analyze the ground state property of this model by varying electron correlation and band filling using the variational Monte Carlo (VMC) method. We calculate the superconducting correlation function, coherence length, superfluid weight, and chemical potential as criteria for BCS-BEC crossover.

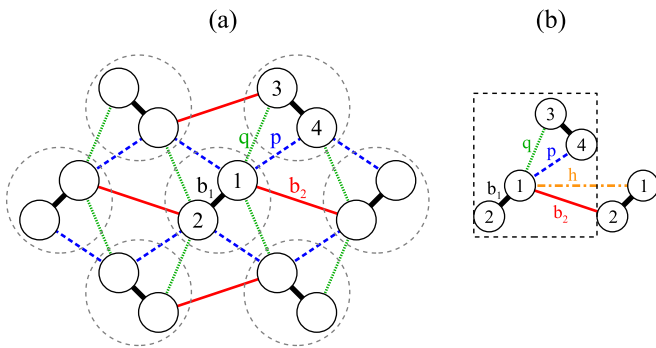


FIG. 1. (a) Schematic lattice structure of the κ -type system. Solid circles represent BEDT-TTF molecules connected by b_1 , b_2 , p , and q bonds. Dashed circles indicate dimers, whose centers form an anisotropic triangular lattice. (b) The unit cell (dashed rectangle) contains four molecules labeled 1, 2, 3, and 4. The h bond exhibits the largest gap for an extended- $s+d_{x^2-y^2}$ type gap function.

Our results indicate that the BCS-BEC crossover can be observed at a hole doping rate of $\delta = 0.06$, where SC persists even in the strongly correlated region due to the absence of competing orders. We also demonstrate transitions to a Mott insulator ($\delta = 0$) and a charge-ordered (stripe) phase ($\delta = 0.11$), both of which mask the BCS-BEC crossover. Our findings align with the observed behavior of real materials and support the feasibility of the BCS-BEC crossover in κ -HgBr and related organic superconductors.

Model and Method— We study the extended Hubbard model defined as [16, 17]

$$H = - \sum_{\langle i,j \rangle \sigma} t_{ij} (c_{i\sigma}^\dagger c_{j\sigma} + \text{H.c.}) + U \sum_i n_{i\uparrow} n_{i\downarrow} + \sum_{\langle i,j \rangle} V_{ij} n_i n_j, \quad (1)$$

where $c_{i\sigma}^\dagger$ ($c_{i\sigma}$) is a creation (annihilation) operator for an electron at the i -th molecular site with spin σ . $n_{i\sigma} = c_{i\sigma}^\dagger c_{i\sigma}$ and $n_i = n_{i\uparrow} + n_{i\downarrow}$ are the number operators, representing the electron number for each spin and total electron number, respectively. U and V_{ij} denote the on-site and intersite Coulomb interactions, respectively. $\langle i,j \rangle$ denotes a pair of neighboring molecules in the κ -type geometry, labeled by b_1 , b_2 , p , and q . As shown in Fig. 1(a), molecules connected by the b_1 bond form dimers (dashed circles), and the centers of these dimers create an anisotropic triangular lattice structure.

A set of transfer integrals t_{ij} is estimated from a first-principles band calculation. However, performing a band calculation for κ -HgBr is challenging due to its nonstoichiometric Hg composition. Instead, we use band calculation results for κ -(BEDT-TTF)₂Cu₂(CN)₃ (κ -CN) [18], which is also a candidate for a QSL [19] and exhibits behavior similar to that of κ -HgBr. The obtained parameters are $(t_{b_1}, t_{b_2}, t_p, t_q) = (199, 91, 85, -17)$ meV = $(1, 0.457, 0.427, -0.085)$ t_{b_1} . In the following, the largest

transfer integral $t = t_{b_1}$ is set as the unit of energy. The unit cell contains four molecules [dashed rectangle in Fig. 1(b)], resulting in a four-band electronic structure. The noninteracting band structure is shown in Fig. S1 of the Supplemental Material [20]. The initial electron density per molecular site is 3/4-filling, or 1/4-filling in a hole picture, which corresponds to 1/2-filling when each dimer is considered a unit (one hole per dimer). To investigate the possibility of BCS-BEC crossover in the κ -type system, we vary the band filling by hole doping and calculate physical quantities relevant to SC.

We employ a VMC method [21–23] to treat the effects of Coulomb interactions. The trial wave function used here is of the Gutzwiller-Jastrow type, $|\Psi\rangle = P_{J_c} P_{J_s} |\Phi\rangle$, where $|\Phi\rangle$ is a one-body state constructed by diagonalizing the one-body Hamiltonian, which includes the superconducting gap $\tilde{\Delta}_{ij}$ and renormalized transfer integrals \tilde{t}_{ij} . P_{J_c} and P_{J_s} represent the charge and spin Jastrow factors, incorporating v_{ij}^c and v_{ij}^s , respectively. The explicit form of $|\Psi\rangle$ are shown in Sec. II of the Supplemental Material [20]. The variational parameters in $|\Psi\rangle$ are optimized simultaneously using the stochastic reconfiguration method [24]. Once $|\Psi\rangle$ is determined, various physical quantities can be calculated.

Result— First, we examine the pair correlation function defined as

$$P_\alpha(\mathbf{r}) = \frac{1}{N_S} \sum_i \langle \Delta_\alpha^\dagger(\mathbf{R}_i) \Delta_\alpha(\mathbf{R}_i + \mathbf{r}) \rangle, \quad (2)$$

where i runs over all molecular sites, N_S is the number of dimers, and $\Delta_\alpha^\dagger(\mathbf{R}_i)$ represents the creation operator for singlet pairs on molecules connected by the α bond,

$$\Delta_\alpha^\dagger(\mathbf{R}_i) = (c_{i\uparrow}^\dagger c_{i+\alpha\downarrow}^\dagger + c_{i+\alpha\uparrow}^\dagger c_{i\downarrow}^\dagger) / \sqrt{2}. \quad (3)$$

If $P_\alpha(\mathbf{r})$ converges to a finite value as $|\mathbf{r}| = r \rightarrow \infty$, superconducting long-range order is present. We calculate $P_\alpha(\mathbf{r})$ up to the 15th-neighbor bond (b_1 , b_2 , p , q , h , \dots), with the largest value taken as the superconducting correlation function $P_{SC} = P_{\alpha_{\max}}(r \rightarrow \infty)$. Our results confirm that the symmetry of the superconducting gap function is of the extended- $s+d_{x^2-y^2}$ type [16, 17, 25–28], and the h bond exhibits the largest gap in real space. Further details on the gap function are provided in Sec. III of the Supplemental Material [20].

Figure 2(a) shows the U/t dependence of P_{SC} for different hole doping rates δ . The ratio between U and intersite Coulomb interactions is fixed as $(V_{b_1}, V_{b_2}, V_p, V_q)/U = (0.5, 0.28, 0.33, 0.29)$, assuming a $1/r$ -dependence [18]. For $\delta = 0$ (576 holes/576 dimers), P_{SC} increases with increasing U/t , displaying BCS-like behavior, and then drops discontinuously to approximately zero at $U/t \approx 7.7$ due to the Mott transition (from SC to a Mott insulator). This corresponds to the pressure-induced Mott transition generally observed in the κ -type system [29]. For $\delta = 0.11$ (640 holes/576

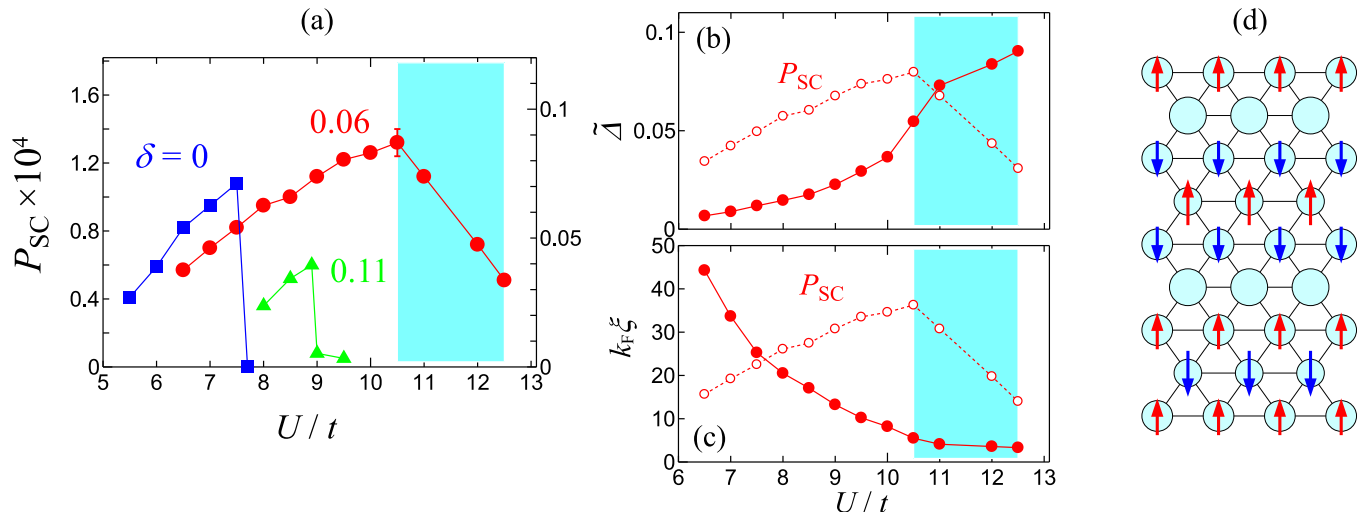


FIG. 2. (a) U/t dependence of the superconducting correlation function P_{SC} for hole doping rates $\delta=0$, 0.06, and 0.11. The corresponding hole densities are 576/576, 608/576, and 640/576 (holes/dimers), respectively, with $N_S = 24 \times 24 = 576$. The blue-shaded area indicates the BCS-BEC crossover region. The statistical errors from Monte Carlo sampling are within the symbol size, except for $U/t = 10.5$. Around $U/t = 10.5$, fluctuations between BCS- and BEC-type states lead to relatively large errors, indicated by the error bar. (b) U/t dependence of the superconducting gap $\hat{\Delta}$. (c) $k_F \xi$ as a function of U/t . (d) Charge and spin configuration of the C4S8 stripe phase stabilized for $U/t > 8.9$ at $\delta = 0.11$. Circles (arrows) represent the total hole (spin) density in each dimer, with radius (length) proportional to the hole (spin) density.

dimers), P_{SC} shows similar behavior to the $\delta = 0$ case. At $U/t \approx 8.9$, a transition to a charge-ordered phase occurs, and P_{SC} decreases discontinuously. The ordering pattern is analogous to the stripe phase observed in cuprate superconductors at $\delta \approx 1/8 = 0.125$ [30, 31]. In this case, the charge periodicity is four and the spin periodicity is eight (C4S8) when each dimer is considered a unit, as shown in Fig. 2(d). Given the similarity to cuprate superconductors [32], it is natural that the stripe phase also appears in the κ -type system at $\delta \approx 1/8$.

In contrast, significantly different behavior is observed for $\delta = 0.06$ (608 holes/576 dimers). Here, P_{SC} increases with increasing U/t and then gradually decreases for $U/t > 10.5$ without any phase transitions. The optimized superconducting gap $\hat{\Delta} = \hat{\Delta}_h$ for $\delta = 0.06$ is also shown in Fig. 2(b). While P_{SC} exhibits a peak structure, $\hat{\Delta}$ increases monotonically with U/t . For $U/t > 10.5$, strong electron correlation suppresses the coherence of Cooper pairs, leading to a decrease in P_{SC} , which is a “true” order parameter of SC ($\sim T_c$), as U/t increases. Meanwhile, $\hat{\Delta}$ reflects a local superconducting correlation and is continuously enhanced by electron correlation. This observed inverse relationship—where local pairing gaps increase as long-range pair coherence decreases—serves as a hallmark of the BCS-BEC crossover. We also plot $k_F \xi = k_F \cdot \hbar v_F / (\pi \hat{\Delta})$ [33] in Fig. 2(c). $k_F \xi$ decreases monotonically with U/t and saturates to approximately $O(1)$, where the coherence length ξ is comparable to the average interparticle distance $\sim 1/k_F$. This behavior reproduces the estimated $k_F \xi$ for κ -HgBr [8] and supports

the occurrence of BCS-BEC crossover.

The BCS-BEC crossover is observable at $\delta = 0.06$ because competing phases are suppressed at this doping level. In square lattice models, SC is often masked by other ordered phases, such as charge and/or spin order, when U/t is large. However, due to the geometrical frustration inherent to a triangular lattice structure, such competing orders are suppressed in the present model. Consequently, SC persists in a strongly correlated region where U/t is sufficiently large to realize the BCS-BEC crossover. For $U/t > 12.5$, an inhomogeneous state emerges, where the variational energy depends on the initial configuration of the Monte Carlo sampling. In this region, phase separation between SC and competing orders, such as Mott insulators or short- and long-range charge-ordered phases, is expected. Indeed, inhomogeneous SC has been observed in κ -HgBr at low-pressure (strongly correlated conditions) [14]. This inhomogeneity results from strong electron correlation effects and resembles the behavior seen in the low-doping regions of cuprate superconductors [34].

We also examine the superfluid weight $D_s \sim n_s/m^*$, where n_s is the superfluid density and m^* is the effective electron mass. D_s is calculated by adding the vector potential \mathbf{A} to the Hamiltonian [Eq. (1)] [35–37] (see Sec. IV in the Supplemental Material for details of the calculation [20]). Figure 3 shows the U/t dependence of D_s/D_s^0 for $\delta = 0$, 0.06, and 0.11, where D_s^0 is the value at $U/t = 0$ for each δ . For $\delta = 0$, D_s/D_s^0 decreases with U/t and goes to zero at the Mott transition. For $\delta = 0.11$,

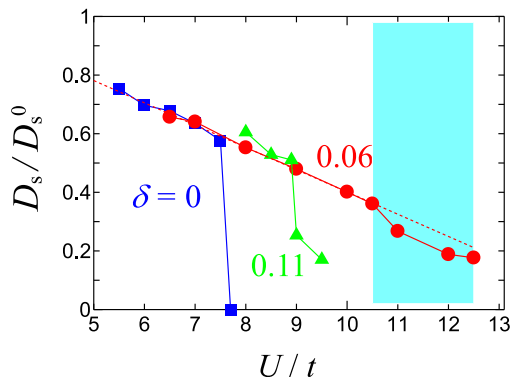


FIG. 3. U/t dependence of the normalized superfluid weight D_s/D_s^0 for $\delta = 0, 0.06$, and 0.11 . D_s^0 is the value at $U/t = 0$ for each δ . The red-dotted line represents the fit for $U/t < 10.5$ and its extrapolation to $U/t > 10.5$. The blue-shaded area indicates the BCS-BEC crossover region.

D_s/D_s^0 also decreases with U/t but jumps to a small, finite value at the first-order transition to the stripe phase, as the electron mobility is suppressed but remains finite. For $\delta = 0.06$, however, D_s/D_s^0 decreases with U/t and shows no discontinuous change across $U/t \approx 10.5$, where P_{SC} exhibits a peak structure, as shown in Fig 2(a). In the BCS regime, all particles contribute to SC, and n_s remains constant. Consequently, D_s/D_s^0 is proportional to $m/m^* \sim z$, where z is the quasiparticle renormalization factor. Indeed, the dependence observed in Fig. 3 aligns with that of z for moderate U/t in previous studies [38, 39], suggesting that the decrease in D_s/D_s^0 is due to an increase in m^* . The deviation from the fit for $U/t > 10.5$ suggests that the additional decrease results from a reduction in n_s , as some particles become incoherent and no longer contribute to SC. This observation also supports the occurrence of the BCS-BEC crossover. We believe that the reduction in P_{SC} likewise results from the decrease in n_s .

The ratio n_s/m^* can be estimated from the magnetic penetration depth λ , with $1/\lambda^2 \sim n_s/m^*$ [40]. The estimated n_s/m^* for κ -HgBr at ambient pressure is $9.4 \times 10^{54} (\text{m}^3\text{kg})^{-1}$, which is one order of magnitude smaller than those of undoped ($\delta = 0$) κ -type superconductors, κ -(BEDT-TTF)₂Cu[N(CN)₂]Br (κ -Br) and κ -(BEDT-TTF)₂Cu(NCS)₂ (κ -NCS) [41]. This low n_s/m^* value for κ -HgBr indicates a heavy electron mass and reduced superfluid density. We propose that κ -HgBr at ambient pressure lies in the BCS-BEC crossover region, where the effect of electron correlation is particularly strong.

The behavior of the fermionic chemical potential μ is one of the criteria for identifying the BCS-BEC crossover. Figure 4 shows the U/t dependence of μ/E_F for $\delta = 0.06$, where E_F is the Fermi energy. Since the electronic carriers in this system are holes, μ and E_F are measured

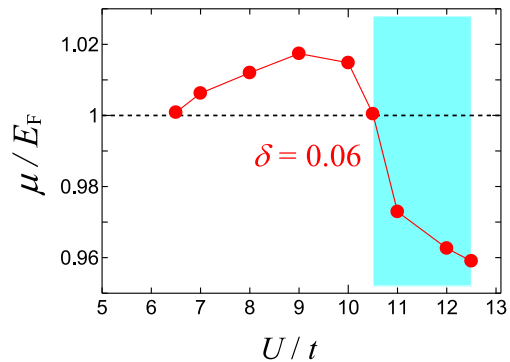


FIG. 4. U/t dependence of the chemical potential μ/E_F for $\delta = 0.06$. The blue-shaded area, where $\mu/E_F < 1$, indicates the BCS-BEC crossover region.

from the band top (see the band structure in Fig. S1 in the Supplemental Material [20]). For $U/t < 10.5$, μ/E_F gradually increases from unity as U/t increases. This behavior reflects electron correlation effects that enhance SC by expanding the Fermi surface area. However, for $U/t > 10.5$, μ/E_F decreases and eventually falls below unity. The decline in μ/E_F suggests that tightly bound pairs begin to decouple from the Fermi surface, leading to pseudogap formation [5]. It can be regarded as a precursor of BCS-BEC crossover. Although μ/E_F remains far from the BEC limit ($\mu/E_F = 0$), we propose that the system enters the BCS-BEC crossover region for $U/t > 10.5$.

Conclusion—Based on the behavior of P_{SC} , $k_F\xi$, D_s/D_s^0 , and μ/E_F , we conclude that the BCS-BEC crossover occurs at $\delta = 0.06$ but not at $\delta = 0$ or $\delta = 0.11$ in the present model. Appropriate hole doping suppresses competing orders, allowing the BCS-BEC crossover to emerge. Most κ -type organic superconductors correspond to $\delta = 0$, where the Mott transition takes place before reaching the BCS-BEC crossover region. In contrast, κ -HgBr, with δ away from zero, has the potential to realize the BCS-BEC crossover. Although the hole doping rate estimated from stoichiometry is $\delta = 0.11$, we anticipate that the charge-ordered phase is suppressed by the effect of Hg^{2+} ions in insulating layers (not included in the present model), which could eventually allow the BCS-BEC crossover to occur in κ -HgBr.

Another way to achieve the BCS-BEC crossover, as we propose, is through hole doping in related materials with $\delta = 0$, such as κ -CN, κ -Br, κ -NCS, and κ -(BEDT-TTF)₂Cu[N(CN)₂]Cl. Systematic experiments varying δ , achievable through techniques such as the electric-double-layer transistor method [42], would be valuable for clarifying the potential for the BCS-BEC crossover in κ -type organic superconductors.

The authors thank K. Kanoda, H. Oike, H. Seo, and S. Imajo for useful discussions. The computation has been done using the facilities of the Supercomputer Center,

Institute for Solid State Physics, University of Tokyo. This work was supported by a Grant-in-Aid for Scientific Research on Innovative Areas “Quantum Liquid Crystals” (KAKENHI Grant No. JP19H05825) from JSPS of Japan, and also supported by JSPS KAKENHI (Grant Nos. JP20K03847 and JP23K25827).

* watanabe.hiroshi@nihon-u.ac.jp

- [1] P. Nozières and S. Schmitt-Rink, Bose condensation in an attractive fermion gas: From weak to strong coupling superconductivity, *J. Low Temp. Phys.* **59**, 195 (1985).
- [2] M. Greiner, C. A. Regal, and D. S. Jin, Emergence of a molecular Bose-Einstein condensate from a Fermi gas, *Nature* **426**, 537 (2003).
- [3] C. A. Regal, M. Greiner, and D. S. Jin, Observation of Resonance Condensation of Fermionic Atom Pairs, *Phys. Rev. Lett.* **92**, 040403 (2004).
- [4] M. Randeria and E. Taylor, Crossover from Bardeen-Cooper-Schrieffer to Bose-Einstein condensation and the unitary Fermi gas, *Annu. Rev. Condens. Matter Phys.* **5**, 209 (2014).
- [5] Q. Chen, J. Stajic, S. Tan, and K. Levin, BCS–BEC crossover: From high temperature superconductors to ultracold superfluids, *Phys. Rep.* **412**, 1 (2005).
- [6] S. Kasahara, T. Watashige, T. Hanaguri, Y. Kohsaka, T. Yamashita, Y. Shimoyama, Y. Mizukami, R. Endo, H. Ikeda, K. Aoyama, T. Terashima, S. Uji, T. Wolf, H. von Löhneysen, T. Shibauchi, Y. Matsuda, Field-induced superconducting phase of FeSe in the BCS-BEC crossover, *Proc. Natl. Acad. Sci. U.S.A.* **111**, 16309 (2014).
- [7] T. Hashimoto, Y. Ota, A. Tsuzuki, T. Nagashima, A. Fukushima, S. Kasahara, Y. Matsuda, K. Matsuura, Y. Mizukami, T. Shibauchi, S. Shin, and K. Okazaki, Bose-Einstein Condensation Superconductivity Induced by Disappearance of the Nematic State, *Sci. Adv.* **6**, eabb9052 (2020).
- [8] Y. Suzuki, K. Wakamatsu, J. Ibuka, H. Oike, T. Fujii, K. Miyagawa, H. Taniguchi, and K. Kanoda, Mott-Driven BEC-BCS Crossover in a Doped Spin Liquid Candidate κ -(BEDT-TTF)₄Hg_{2.89}Br₈, *Phys. Rev. X* **12**, 011016 (2022).
- [9] Y. Nakagawa, Y. Kasahara, T. Nomoto, R. Arita, T. Nojima, and Y. Iwasa, Gate-controlled BCS-BEC crossover in a two-dimensional superconductor, *Science* **372**, 190 (2021).
- [10] Q. J. Chen, Z. Q. Wang, R. Boyack, S. L. Yang, and K. Levin, When superconductivity crosses over: From BCS to BEC, *Rev. Mod. Phys.* **96**, 025002 (2024).
- [11] N. Witt, Y. Nomura, S. Brener, R. Arita, A. I. Lichtenstein, and T. O. Wehling, Bypassing the lattice BCS-BEC crossover in strongly correlated superconductors: resilient coherence from multiorbital physics, arXiv:2310.09063.
- [12] R. N. Lyubovskaya, E. A. Zhilyaeva, A. V. Zvarykina, V. N. Laukhin, R. B. Lyubovskii, and S. I. Pesotskii, Is the organic metal (ET)₄Hg₃Br₈ a quasi-2D superconductor?, *JETP Lett.* **45**, 530 (1987).
- [13] R. N. Lyubovskaya, E. I. Zhilyaeva, S. I. Pesotskii, R. B. Lyubovskii, L. O. Atovmyan, O. A. D’yachenko, and T. G. Takhirov, Superconductivity of (ET)₄Hg_{2.89}Br₈ at atmospheric pressure and $T_c = 4.3\text{K}$ and the critical-field anisotropy, *JETP Lett.* **46**, 188 (1987).
- [14] H. Oike, K. Miyagawa, H. Taniguchi, and K. Kanoda, Pressure-Induced Mott Transition in an Organic Superconductor with a Finite Doping Level, *Phys. Rev. Lett.* **114**, 067002 (2015).
- [15] H. Oike, Y. Suzuki, H. Taniguchi, Y. Seki, K. Miyagawa, and K. Kanoda, Anomalous Metallic Behaviour in the Doped Spin Liquid Candidate κ -(ET)₄Hg_{2.89}Br₈, *Nat. Commun.* **8**, 756 (2017).
- [16] H. Watanabe, H. Seo, and S. Yunoki, Phase Competition and Superconductivity in κ -(BEDT-TTF)₂X: Importance of Intermolecular Coulomb interactions, *J. Phys. Soc. Jpn.* **86**, 033703 (2017).
- [17] H. Watanabe, H. Seo, and S. Yunoki, Mechanism of superconductivity and electron-hole doping asymmetry in κ -type molecular conductors, *Nat. Commun.* **10**, 3167 (2019).
- [18] T. Koretsune and C. Hotta, Evaluating model parameters of the κ - and β' -type Mott insulating organic solids, *Phys. Rev. B* **89**, 045102 (2014).
- [19] Y. Shimizu, K. Miyagawa, K. Kanoda, M. Maesato, and G. Saito, Spin Liquid State in an Organic Mott Insulator with a Triangular Lattice, *Phys. Rev. Lett.* **91**, 107001 (2003).
- [20] See Supplemental Material.
- [21] W. L. McMillan, Ground State of Liquid He⁴, *Phys. Rev.* **138**, A442 (1965).
- [22] D. Ceperley, G. V. Chester, and M. H. Kalos, Monte Carlo simulation of a many-fermion study, *Phys. Rev. B* **16**, 3081 (1977).
- [23] H. Yokoyama and H. Shiba, Variational Monte-Carlo Studies of Hubbard Model. I, *J. Phys. Soc. Jpn.* **56**, 1490 (1987).
- [24] S. Sorella, Generalized Lanczos algorithm for variational quantum Monte Carlo, *Phys. Rev. B* **64**, 024512 (2001); S. Yunoki and S. Sorella, Two spin liquid phases in the spatially anisotropic triangular Heisenberg model, *ibid.* **74**, 014408 (2006).
- [25] B. J. Powell and R. H. McKenzie, Symmetry of the superconducting order parameter in frustrated systems determined by the spatial anisotropy of spin correlations, *Phys. Rev. Lett.* **98**, 027005 (2007).
- [26] K. Kuroki, T. Kimura, R. Arita, Y. Tanaka, and Y. Matsuda, $d_{x^2-y^2}$ - versus d_{xy} - like pairings in organic superconductors κ -(BEDT-TTF)₂X, *Phys. Rev. B* **65**, 100516(R) (2002).
- [27] D. Guterding, S. Diehl, M. Altmeyer, T. Methfessel, U. Tutsch, H. Schubert, M. Lang, J. Müller, M. Huth, H. O. Jeschke, R. Valentí, M. Jourdan, and H.-J. Elmers, Near-degeneracy of extended $s + d_{x^2-y^2}$ and d_{xy} order parameters in quasi-two-dimensional organic superconductors *Phys. Rev. Lett.* **116**, 237001 (2016).
- [28] K. Zantout, M. Altmeyer, S. Backes, and R. Valentí, Superconductivity in correlated BEDT-TTF molecular conductors: Critical temperatures and gap symmetries, *Phys. Rev. B* **97**, 014530 (2018).
- [29] K. Kanoda, Metal–Insulator Transition in κ -(ET)₂X and (DCNQI)₂M: Two Contrasting Manifestation of Electron Correlation, *J. Phys. Soc. Jpn.* **75**, 051007 (2006).
- [30] J. M. Tranquada, B. J. Sternlieb, J. D. Axe, Y. Nakamura, and S. Uchida, Evidence for stripe correlations of spins and holes in copper oxide superconductors, *Nature* **375**, 561 (1995).

- [31] H. Watanabe, T. Shirakawa, K. Seki, H. Sakakibara, T. Kotani, H. Ikeda, and S. Yunoki, Monte Carlo study of cuprate superconductors in a four-band d - p model: role of orbital degrees of freedom, *J. Phys.: Condens. Matter* **35**, 195601 (2023).
- [32] R. H. McKenzie, Similarities Between Organic and Cuprate Superconductors, *Science* **278**, 820 (1997).
- [33] A. Paramekanti, M. Randeria, and N. Trivedi, High- T_c superconductors: A variational theory of the superconducting state, *Phys. Rev. B* **70**, 054504 (2004).
- [34] V. J. Emery and S. A. Kivelson, Frustrated electronic phase separation and high-temperature superconductors, *Physica C* **209**, 597 (1993).
- [35] A. J. Millis and S. N. Coppersmith, Variational wave functions and the Mott transition, *Phys. Rev. B* **43**, 13770 (1991).
- [36] D. J. Scalapino, S. R. White, and S. C. Zhang, Insulator, metal, or superconductor: The criteria, *Phys. Rev. B* **47**, 7995 (1993).
- [37] S. Tamura and H. Yokoyama, Drude and Superconducting Weights and Mott Transition in Variation Theory, *J. Phys. Soc. Jpn.* **84**, 064707 (2015).
- [38] J. Merino, B. J. Powell, and R. H. McKenzie, Ferromagnetism, paramagnetism, and a Curie-Weiss metal in an electron-doped Hubbard model on a triangular lattice, *Phys. Rev. B* **73**, 235107 (2006).
- [39] T. Watanabe, H. Yokoyama, Y. Tanaka, and J. Inoue, Superconductivity and a Mott Transition in a Hubbard Model on an Anisotropic Triangular Lattice, *J. Phys. Soc. Jpn.* **75**, 074707 (2006).
- [40] Y. J. Uemura, L. P. Le, G. M. Luke, B. J. Sternlieb, W. D. Wu, J. H. Brewer, T. M. Riseman, C. L. Seaman, M. B. Maple, M. Ishikawa, D. G. Hinks, J. D. Jorgensen, G. Saito, and H. Yamochi, Basic Similarities among Cuprate, Bismuthate, Organic, Chevrel-Phase, and Heavy-Fermion Superconductors Shown by Penetration-Depth Measurements, *Phys. Rev. Lett.* **66**, 2665 (1991).
- [41] K. Wakamatsu, Y. Ueno, K. Miyagawa, H. Taniguchi, and K. Kanoda, Reduced superfluid density in a doped spin liquid candidate, arXiv: 2205.03682.
- [42] Y. Kawasugi, K. Seki, Y. Edagawa, Y. Sato, J. Pu, T. Takenobu, S. Yunoki, H. M. Yamamoto, and R. Kato, Electron-hole doping asymmetry of Fermi surface reconstructed in a simple Mott insulator, *Nat. Commun.* **7**, 12356 (2016).

Supplemental Material for “Possibility of BCS-BEC crossover in κ -ET organic superconductors”

Hiroshi Watanabe^{1,2,*} and Hiroaki Ikeda³

¹*Department of Liberal Arts and Basic Sciences,
College of Industrial Technology, Nihon University, Chiba 275-8576, Japan*

²*Research Organization of Science and Technology, Ritsumeikan University, Shiga 525-8577, Japan*

³*Department of Physical Science, Ritsumeikan University, Shiga 525-8577, Japan*

(Dated: November 26, 2024)

I. BAND STRUCTURE

The noninteracting band structure and the Fermi surface for κ -HgBr are shown in Fig. S1. The upper two bands (bands 1 and 2) contribute to the formation of the Fermi surface. The unit cell in real space is $R_x \times 2R_y$ rectangle [Fig. 1(b) in the main text], where $R_y = 0.7R_x$.

II. TRIAL WAVE FUNCTION

The one-body part $|\Phi\rangle$ of a trial wave function for superconductivity (SC) is obtained from the Bogoliubov de-Genes (BdG) type Hamiltonian in real space,

$$H_{\text{BdG}} = \sum_{i,j} \begin{pmatrix} c_{i\uparrow}^\dagger & c_{i\downarrow} \end{pmatrix} \begin{pmatrix} T_{ij\uparrow} & \tilde{\Delta}_{ij} \\ \tilde{\Delta}_{ji} & -T_{ji\downarrow} \end{pmatrix} \begin{pmatrix} c_{j\uparrow} \\ c_{j\downarrow}^\dagger \end{pmatrix}, \quad (\text{S1})$$

where $\sum_{i,j}$ runs over all molecular sites. $T_{ij\sigma}$ represents the normal part, including renormalized transfer integrals \tilde{t}_{ij} and the chemical potential μ . Here, μ is a variational parameter and deviates from the Fermi energy E_F due to electron correlation effects. $\tilde{\Delta}_{ij}$ represents the superconducting gap in real space, forming the anomalous part of the Hamiltonian. Therefore, the variational parameters to be optimized in $|\Phi\rangle$ are \tilde{t}_{ij} , μ , and $\tilde{\Delta}_{ij}$ with $\tilde{t}_{b_1} = t$ fixed as

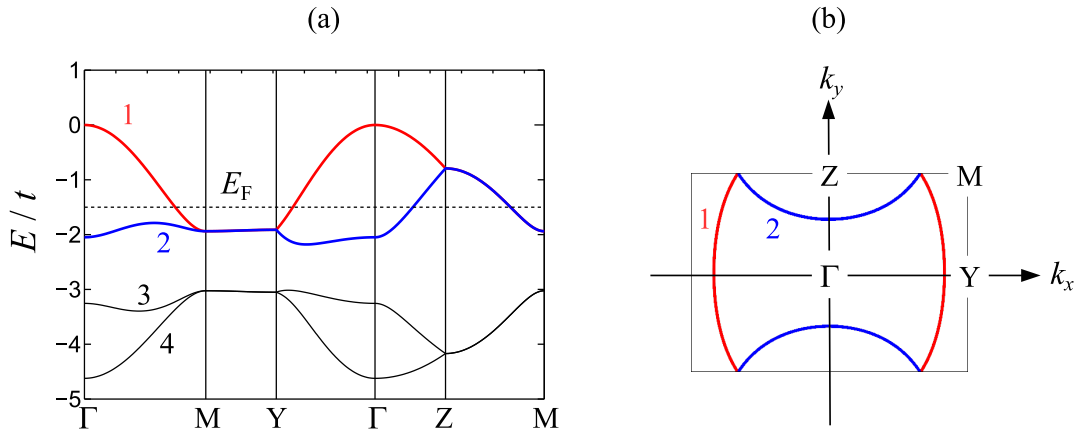


FIG. S1. (a) Band structure and (b) Fermi surface for κ -HgBr. High symmetry points are $\Gamma(0,0)$, $Y(\pi/R_x)$, $Z(\pi/2R_y)$, and $M(\pi/R_x, \pi/2R_y)$.

* watanabe.hiroshi@nihon-u.ac.jp

the unit of energy. In this study, pairing interactions are considered between bonds up to the 15th neighbor (e.g., b_1 , b_2 , p , q , h , \dots). Setting $\tilde{\Delta}_{ij} = 0$ yields the paramagnetic phase.

The charge and spin Jastrow factors are defined as

$$P_{J_c} = \exp\left[-\sum_{i,j} v_{ij}^c n_i n_j\right], \quad (\text{S2})$$

and

$$P_{J_s} = \exp\left[-\sum_{i,j} v_{ij}^s s_i^z s_j^z\right], \quad (\text{S3})$$

where $\sum_{i,j}$ runs over all molecular sites. These factors control long-range charge and spin correlations, respectively. The variational parameters to be optimized are v_{ij}^c and v_{ij}^s . Here, we do not include mean-field type charge and spin gaps, as they often lead to overestimations of charge and spin orders. The Mott insulating and stripe phases observed in the main text arise from the effects of P_{J_c} and P_{J_s} .

III. SUPERCONDUCTING GAP FUNCTION

In κ -type organic superconductors, the degree of geometrical frustration is an important parameter for both SC and magnetic orders. In the dimer approximation, the ratio between the effective diagonal and horizontal interdimer transfer integrals is estimated as $|t'_{\text{eff}}/t_{\text{eff}}| \sim |t_{b_2}|/(|t_p| + |t_q|)$. A value of $|t'_{\text{eff}}/t_{\text{eff}}| \approx 1$ indicates strong geometrical frustration (triangular-lattice-like), whereas $|t'_{\text{eff}}/t_{\text{eff}}| \ll 1$ suggests weak geometrical frustration (square-lattice-like). The primary proposed symmetries for SC in κ -type organic superconductors are extended- $s+d_{x^2-y^2}$ and d_{xy} . The former symmetry is favored in systems with strong geometrical frustration, while the latter is favored in systems with weak geometrical frustration. The competition between these symmetries is discussed in detail in our previous study [1].

The quantum spin liquid candidates κ -HgBr and κ -CN are expected to exhibit extended- $s+d_{x^2-y^2}$ symmetry due to their strong geometrical frustration. In \mathbf{k} -space representation, the main contribution of the gap function for the extended- $s+d_{x^2-y^2}$ type is given as [1]

$$\Delta^\alpha = \Delta_1^\alpha \left[\cos\left(\frac{1}{2}k_x R_x + k_y R_y\right) + \cos\left(\frac{1}{2}k_x R_x - k_y R_y\right) \right] + \Delta_2^\alpha \cos k_x R_x, \quad (\text{S4})$$

where $\alpha (= 1, 2)$ denotes the band index shown in Fig. S1. The optimized $\tilde{\Delta}_{ij}$ in this study changes sign four times in real space, which is consistent with the extended- $s+d_{x^2-y^2}$ type.

IV. SUPERFLUID WEIGHT

To calculate the superfluid weight, we add the vector potential to the kinetic energy term in the Hamiltonian (1) in the main text as follows,

$$H(A) = -\sum_{\langle i,j \rangle \sigma} \left[t_{ij}(A) c_{i\sigma}^\dagger c_{j\sigma} + \text{H.c.} \right] + U \sum_i n_{i\uparrow} n_{i\downarrow} + \sum_{\langle i,j \rangle} V_{ij} n_i n_j, \quad (\text{S5})$$

where $t_p \rightarrow t_p e^{\pm iA}$ as shown in Fig. S2. Here, A corresponds to the Peierls phase and induces a current along the p bond. Using the VMC method, the Drude weight is estimated as

$$D = \left. \frac{\partial^2 E(A)}{\partial A^2} \right|_{A=0}, \quad (\text{S6})$$

where $E(A)$ is a variational energy for $H(A)$. When the system is insulating, $D = 0$ because the energy increase induced by an infinitesimal A is suppressed due to the lack of free carriers, preventing the response to the external field. However, as pointed out by Millis and Coppersmith [3], D cannot be exactly zero (i.e., the system appears metallic) as long as the trial wave function is real.

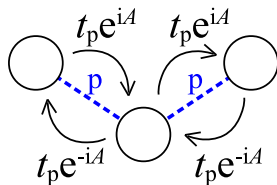


FIG. S2. Schematic picture of hopping processes with additional phase factors $e^{\pm iA}$.

To address this issue, we introduce a complex phase factor in the trial wave function [4] defined as

$$P_{\theta}^{\text{dim}} = \exp \left[i \sum_{(m,n)} \theta_{mn} d_m^{\text{dim}} h_n^{\text{dim}} \right], \quad (\text{S7})$$

where $\sum_{(m,n)}$ runs over nearest-neighbor dimer pair connected by p bonds. Here, $d_m^{\text{dim}} = n_{m_1\uparrow}n_{m_1\downarrow} + n_{m_2\uparrow}n_{m_2\downarrow}$ is the total number of doublons in the m -th dimer, and $h_n^{\text{dim}} = (1 - n_{n_1\uparrow})(1 - n_{n_1\downarrow}) + (1 - n_{n_2\uparrow})(1 - n_{n_2\downarrow})$ is the total number of holons in the n -th dimer. In essence, P_{θ}^{dim} introduces a phase to the configuration of neighboring doublon-holon pairs. We assume a simple form for θ_{mn} as

$$\theta_{mn} = \begin{cases} -\theta & x_m - x_n > 0 \\ \theta & x_m - x_n < 0 \end{cases} \quad (\text{S8})$$

where θ is a variational parameter. Through this factor, hopping processes that create or annihilate doublon-holon pairs acquire the complex phase $e^{\pm i(A-\theta)}$, where θ works to counteract the effect of A .

The superfluid density D_s is also estimated using Eq. (S6) for superconducting trial wave functions [2, 4, 5]. Figure S3 shows the A dependence of the energy increase $\Delta E(A) = E(A) - E(0)$ for $U/t = 5.5$ and $U/t = 7.7$. For $U/t = 5.5$, $\Delta E(A)$ exhibits a quadratic increase with respect to A , and $D_s \approx 0.35$ can be estimated from the coefficient. In contrast, for $U/t = 7.7$, $\Delta E(A) \sim A^3$, and $D_s \rightarrow 0$ as $A \rightarrow 0$. Based on the A dependence of $\Delta E(A)$, we conclude that the system is superconducting for $U/t = 5.5$, while it is nonsuperconducting and insulating for $U/t = 7.7$, despite the fact that the optimized $\tilde{\Delta}_{ij}$ remains finite. This conclusion is further supported by the superconducting correlation function P_{SC} in Fig. 2(a) of the main text.

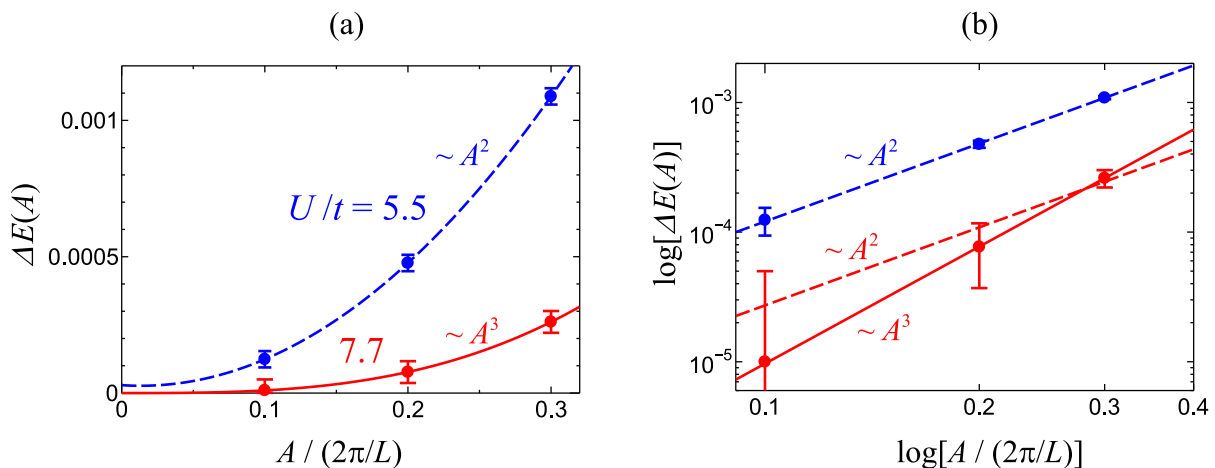


FIG. S3. A dependence of the energy increase $\Delta E(A) = E(A) - E(0)$ for $U/t = 5.5$ and $U/t = 7.7$. (a) in linear scale and (b) in logarithmic scale. Solid (dashed) curves represent A^3 (A^2) fitting.

The reason why the variational phase factor P_{θ}^{dim} effectively describes the insulating phase is as follows. In the Mott insulating phase, most of the kinetic energy arises from hopping processes that create or annihilate doublon-holon pairs, as these pairs are strongly bound and free carriers are absent. Therefore, if θ is optimized to satisfy $\theta \approx A$, the energy increase induced by A would be nearly canceled out. Indeed, as shown in Fig. S3, most of the energy

increase is canceled for $U/t = 7.7$ with the optimized $\theta/A \approx 0.8$. Although improvements to P_θ^{dim} , such as introducing long-range doublon-holon phase factors, may yield even better results, we believe that the simple form in Eq. (S8) captures the essential physics of conducting phenomena in strongly correlated electron systems.

-
- [1] H. Watanabe, H. Seo, and S. Yunoki, Mechanism of superconductivity and electron-hole doping asymmetry in κ -type molecular conductors, *Nat. Commun.* **10**, 3167 (2019).
 - [2] D. J. Scalapino, S. R. White, and S. C. Zhang, Insulator, metal, or superconductor: The criteria, *Phys. Rev. B* **47**, 7995 (1993).
 - [3] A. J. Millis and S. N. Coppersmith, Variational wave functions and the Mott transition, *Phys. Rev. B* **43**, 13770 (1991).
 - [4] S. Tamura and H. Yokoyama, Drude and Superconducting Weights and Mott Transition in Variation Theory, *J. Phys. Soc. Jpn.* **84**, 064707 (2015).
 - [5] B. Hetényi, Drude Weight, Meissner Weight, Rotational Inertia of Bosonic Super fluids: How Are They Distinguished?, *J. Phys. Soc. Jpn.* **83**, 034711 (2014).